FARADAY

Complexation of Methyl Orange and Tropaeolin 000 No. 2 by β-cyclodextrin dimers

Carolyn A. Haskard,[a] Bruce L. May,[a] Tomas Kurucsev,[a] Stephen F. Lincoln[a]* and Christopher J. Easton[b]

[a] *Department of Chemistry, University of Adelaide, South Australia 5005, Australia*

[b] *Research School of Chemistry, Australian National University, Canberra, ACT 0200, Australia*

Spectrophotometric studies of the complexation of Methyl Orange (MO^-) and Tropaeolin 000 No. 2 (TR^-) anions by dimeric *N*,*N*′-bis(6^A-deoxy-6^A-β-cyclodextrin)urea $(\beta CD)_2ur$ and its oxalamide and succinamide analogues, $(\beta CD)_2ox$ and $(\beta CD)_2su$, respectively, are consistent with the predominant formation of complexes of the general formulae $(\beta CD)_2x \cdot MO^-$ characterized by stability constants $K_1 = (1.05 \pm 0.04) \times 10^5$, $(1.92 \pm 0.04) \times 10^5$ and $(2.50 \pm 0.02) \times 10^4$ dm^3 mol^{-1} and $(\beta CD)_2x \cdot TR^-$ characterized by $K_1 = (1.39 \pm 0.03) \times 10^4$, $(7.4 \pm 0.1) \times 10^3$ and $(4.60 \pm 0.05) \times 10^3$ dm^3 mol^{-1}, in aqueous phosphate buffer at pH 9.0 and 5.5 and 298.2 K. These values are significantly greater than $K_1 = 2160$ and 710 dm^3 mol^{-1} for the β-cyclodextrin complexes, $\beta CD \cdot MO^-$ and $\beta CD \cdot TR^-$ and are indicative of cooperative binding in $(\beta CD)_2x \cdot MO^-$ and $(\beta CD)_2x \cdot TR^-$. The factors affecting complex stability are discussed and comparisons are made with related systems.

β-Cyclodextrin (βCD) is produced from the enzymatic degradation of starch, and is the cyclic α-1,4-linked heptamer of glucopyranose in which seven primary and fourteen secondary hydroxy groups, respectively, delineate the narrow and wide ends of a macrocyclic annulus whose hydrophobic interior is lined with methine and methylene groups and ether oxygens.[1–3] This hydrophobic interior functions as a recognition site when βCD acts as the host in the formation of $\beta CD \cdot G$ host–guest complexes with a wide range of guests (G), most of which contain an aromatic group which enters the hydrophobic region of the βCD annulus on complexation.[4–6] When two βCD are joined through a linker, x, in a dimer, $(\beta CD)_2x$,[7–9] the stability of the host–guest complex, $(\beta CD)_2x \cdot G$, in which G has two aromatic binding sites, is usually substantially increased over that of $\beta CD \cdot G$.[7,8,10–20] This is attributable to cooperation between the two βCD recognition sites in complexing G in $(\beta CD)_2x \cdot G$. We now seek further insight into this cooperative effect through a study of the influence of the variation of the linker length in the β-cyclodextrin dimers *N*,*N*′-bis-(6^A-deoxy-6^A-β-cyclodextrin)-urea, $(\beta CD)_2ur$, and its oxalamide [$(\beta CD)_2ox$] and succinamide [$(\beta CD)_2su$] analogues[9] on the binding of the anions of Methyl Orange and Tropaeolin 000 No. 2. Both dyes possess one phenylsulfonate binding site but their second binding sites are phenyl and naphthyl groups, respectively, (Fig. 1) which facilitate an assessment of the effect of guest structural variation on complexation.

Experimental

The dimer β-cyclodextrins, $(\beta CD)_2x$, were prepared by methods similar to those reported in the literature[9] and were shown to be >95% pure by microanalysis, thin layer chromatography (TLC) and ^1H and ^{13}C NMR spectroscopy. The minor impurity was βCD. The $(\beta CD)_2x$ were dried to constant weight and stored over P_2O_5 in vacuum desiccators in the dark prior to use. Methyl Orange (BDH) was used as supplied. Tropaeolin 000 No. 2 (BDH) was purified by salting out from hot water using sodium acetate, after which it was recrystallized three times from water and then twice from ethanol. Deionized water, purified with a MilliQ-Reagent system to produce water with a specific resistance of > 15 MΩ cm, was used in the preparation of all solutions immediately prior to measurement.

Methyl Orange, Tropaeolin 000 No. 2 and $(\beta CD)_2x$ solutions were prepared in aqueous 0.100 mol dm^{-3} Na_2HPO_4 and 0.020 mol dm^{-3} K_2SO_4 adjusted to pH 9.0 and 5.5, respectively, with either NaOH or H_2SO_4, under which conditions both dyes existed in their anionic forms MO^- and TR^-.[21,22] Total $[MO^-]$ was constant at 3.8×10^{-5} mol

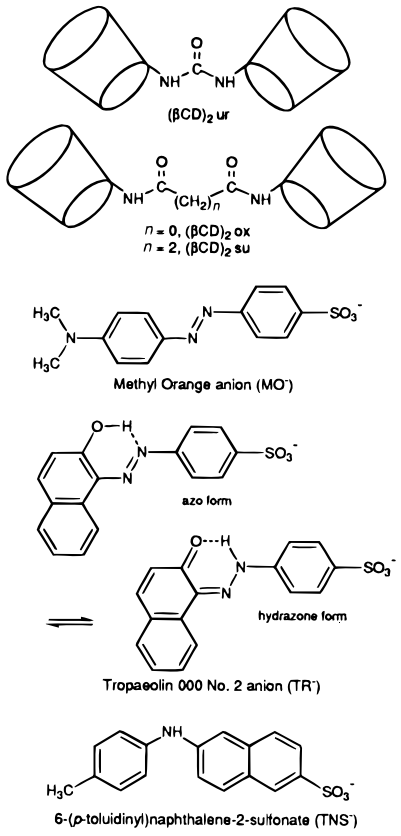

Fig. 1 Schematic illustrations of the β-cyclodextrin dimers, $(\beta CD)_2x$, where the cyclodextrin annulus is represented by a truncated cone in which the narrow end is delineated by six primary hydroxy groups and a secondary amine group, and the wide ends delineated by fourteen secondary hydroxy groups. The structures of Methyl Orange anion MO^-, Tropaeolin 000 No. 2 anion, TR^- and of 6-(*p*-toluidinyl) naphthalene-2-sulfonate, TNS^-, are also shown.

dm^{-3} for the $(\beta CD)_2ur$ studies and 4.0×10^{-5} mol dm^{-3} for the $(\beta CD)_2ox$ and $(\beta CD)_2su$ studies. Total $[(\beta CD)_2ur]$ was varied in the range (1.81×10^{-6})–(2.66×10^{-4}) mol dm^{-3} (21 solutions), $[(\beta CD)_2ox]$ in the range (2.80×10^{-6})–(1.00×10^{-2}) mol dm^{-3} (28 solutions) and $[(\beta CD)_2su]$ in the range (8.12×10^{-6})–(8.01×10^{-3}) mol dm^{-3} (28 solutions) in the spectrophotometric MO^- complexation studies. Total $[TR^-]$ was constant at 4.1×10^{-5}, 3.7×10^{-5} and 4.0×10^{-5} mol dm^{-3} for the $(\beta CD)_2ur$, $(\beta CD)_2ox$ and $(\beta CD)_2su$ studies, respectively. Total $[(\beta CD)_2ur]$ was varied in the range (3.86×10^{-6})–(3.73×10^{-4}) mol dm^{-3} (29 solutions), $[(\beta CD)_2ox]$ in the range (9.47×10^{-6})–(3.20×10^{-3}) mol dm^{-3} (29 solutions) and $[(\beta CD)_2su]$ in the range (2.38×10^{-5})–(4.93×10^{-3}) mol dm^{-3} (36 solutions) for the TR^- complexation studies.

Stability constants for the MO^- complexes formed with $(\beta CD)_2x$ were determined from data in the range 410–440 and 464–520 nm for $(\beta CD)_2ur$, 404–446 and 464–520 nm for $(\beta CD)_2ox$ and 404–444 and 464–520 nm for $(\beta CD)_2su$. Stability constants for the TR^- complexes formed with $(\beta CD)_2x$ were determined from data in the range 450–510 nm for $(\beta CD)_2ur$, 440–492 nm $(\beta CD)_2ox$ and 450–510 nm for $(\beta CD)_2su$. All data fitting was carried out on a AcerPower 466d computer using a non-linear least-squares regression analysis program based on Method 5 of Pitha and Jones.[23] Absorbance spectra were run at 298.2 ± 0.1 K in 1 cm pathlength matched quartz cells on a Zeiss DMR 10 spectrophotometer against reference solutions containing all components of the solution of interest except the dye. Spectra were digitized at 2 nm intervals over the range 350–550 nm.

Aggregation of MO^- [24] and TR^- [25,26] is reported to occur in aqueous solution, as evidenced by a decrease from a linear absorption increase as $[MO^-]$ and $[TR^-]$, respectively, increase. No departures from Beer's law were observed up to the $[MO^-]$ and $[TR^-]$ used in this study.

Results

Complexation of MO^- by $(\beta CD)_2x$

The variation of the MO^- absorption spectrum with $[(\beta CD)_2x]$ is exemplified by the montage shown in Fig. 2 for the $MO^-/(\beta CD)_2su$ system. Those observed as total $[(\beta CD)_2ur]$, and $[(\beta CD)_2ox]$ are varied, are similar. An isosbestic point is observed at 388 nm for the $MO^-/(\beta CD)_2su$ system [compared with 390 nm for both the $MO^-/(\beta CD)_2ur$ and $MO^-/(\beta CD)_2ox$ systems] and a second, less well defined, isosbestic point is observed at 451–453 nm which compares with 448–454 and 453–457 nm for the $MO^-/(\beta CD)_2ur$ and $MO^-/(\beta CD)_2ox$ systems. These variations are consistent with the presence of two predominant environments for MO^- [eqn. (1)] where $(\beta CD)_2x \cdot MO^-$ is a host–guest complex. The fitting of the absorbance data for each system to the algorithm for the variation of MO^- absorption with total $[(\beta CD)_2x]$ for the equilibrium shown in eqn. (1), exemplified by the $MO^-/(\beta CD)_2su$ system in Fig. 3, yields the K_1 values in Table 1. The small variation in wavelength in the longer-wavelength isosbestic point may arise from experimental error or the presence of a small amount of a second complex which could be $(\beta CD)_2x \cdot (MO)_2^{2-}$ in which the MO^- dimer is complexed as shown in eqn. (2).

$$(\beta CD)_2x + MO^- \overset{K_1}{\rightleftharpoons} (\beta CD)_2x \cdot MO^- \quad (1)$$

$$(\beta CD)_2x \cdot MO^- + MO^- \overset{K_2}{\rightleftharpoons} (\beta CD)_2x \cdot (MO)_2^{2-} \quad (2)$$

The absorption data for all three systems were fitted to the algorithm for the variation of MO^- absorption with total $[(\beta CD)_2x]$ arising from the combined equilibria shown in eqn. (1) and (2), and derived K_1 and K_2 appear in Table 1. The errors in K_2 are large and those in K_1 are greater than those obtained when the data were fitted to the algorithm arising from the equilibrium shown in eqn. (1) alone, but the sum of the squares of the residuals (ssr) for the overall data fits decrease. However, over the ranges of total $[MO^-]$ and $[(\beta CD)_2x]$ studied, the maximum percentages of MO^- existing in the free MO^-, $(\beta CD)_2x \cdot MO^-$ and $(\beta CD)_2x \cdot (MO)_2^{2-}$ environments as $[(\beta CD)_2x]$ is varied are 83.7, 99.6 and 5.7% for the $(\beta CD)_2su$ system, 93.5, 100.0 and 0.4% for the $(\beta CD)_2ox$ system, and 95.7, 96.8 and 0.6% for the $(\beta CD)_2ur$ system, as calculated from the simultaneously fitting of the data to eqn. (1) and (2). Thus, $(\beta CD)_2x \cdot (MO)_2^{2-}$ is not a significant species under the conditions of this study.

The formation of $\beta CD \cdot MO^-$ [eqn. (3)] is characterized by K_1 in the range (2.16×10^3)–(4.88×10^3) dm^3 mol^{-1}, a variation which is attributable to the differing experimental conditions and data treatments employed in the reported studies.[7,27–33] A value of $K_1 = 2.16 \times 10^3$ dm^3 mol^{-1} was determined under identical conditions to this study.[21] Some studies have also detected $\beta CD \cdot (MO)_2^{2-}$ [eqn. (4)] for which values of $K_2 = 606$ and 600 dm^3 mol^{-1} have been determined.[7,25] It is seen from these data that $(\beta CD)_2x \cdot MO^-$ is much more stable than is $\beta CD \cdot MO^-$ consistent with the strength of cooperative binding varying in the sequence $(\beta CD)_2ox \cdot MO^- > (\beta CD)_2ur \cdot MO^- > (\beta CD)_2su \cdot MO^-$.

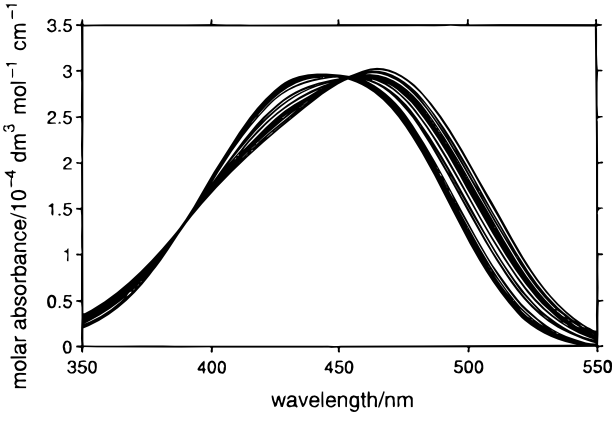

Fig. 2 Absorbance variation of MO^- $(4.0 \times 10^{-5}$ mol $dm^{-3})$ with $[(\beta CD)_2su]$ in the range (8.12×10^{-6})–(8.01×10^{-3}) mol dm^{-3} in aqueous phosphate buffer at pH 9.0 and 298.2 K. The MO^- absorbance decreases with increase in $[(\beta CD)_2su]$ from 350 nm to the first isosbestic point and from the second isosbestic point to 550 nm. Between the isosbestic points MO^- absorbance increases with increase in $[(\beta CD)_2su]$.

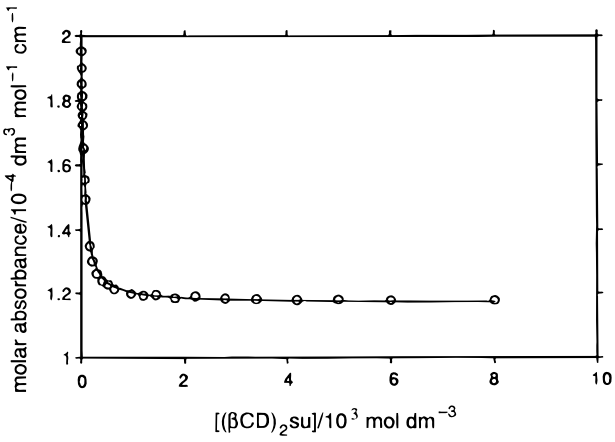

Fig. 3 Absorbance variation of MO^- with $[(\beta CD)_2su]$ at 500 nm under the same conditions as for Fig. 2. The solid curve represents the best fit of the data, collected at 2 nm intervals in the range 404–444 and 464–520 nm, to the algorithm arising from the equilibrium shown in eqn. (1).

Table 1 Stability constants for βCD and $(\beta CD)_2x$ complexes of MO^-, TR^- and TNS^- in aqueous phosphate buffer at pH 9.0, 5.5 and 7.0, respectively, and 298.2 K

host	guest	$K_1/10^{-3}$ dm^3 mol^{-1} [a]	$K_2/10^{-3}$ dm^3 mol^{-1} [a]	10^{-2} ssr[b]
βCD	MO^-	2.16[c]		
$(\beta CD)_2$su	MO^-	25.0 ± 0.2[d]		11.8
$(\beta CD)_2$ox	MO^-	192 ± 4[d]		50.0
$(\beta CD)_2$ur	MO^-	105 ± 4[d]		50.0
$(\beta CD)_2$su	MO^-	46 ± 2[e]	8 ± 2[e]	6.5
$(\beta CD)_2$ox	MO^-	240 ± 30[e]	0.9 ± 3.1[e]	32.5
$(\beta CD)_2$ur	MO^-	150 ± 20[e]	2 ± 5[e]	31.6
βCD	TR^-	0.71 ± 0.07[f]	4000 ± 7000[f]	
$(\beta CD)_2$su	TR^-	4.60 ± 0.05[g]		4.50
$(\beta CD)_2$ox	TR^-	7.4 ± 0.1[g]		1.97
$(\beta CD)_2$ur	TR^-	13.9 ± 0.3[g]		3.17
$(\beta CD)_2$su	TR^-	3.1 ± 0.6[h]	6 ± 2[h]	3.75
$(\beta CD)_2$ox	TR^-	140 ± 20[h]	390 ± 80[h]	1.19
$(\beta CD)_2$ur	TR^-	51 ± 8[h]	160 ± 50[h]	2.68
βCD	TNS^-	3.14 ± 0.02[i]	0.086 ± 0.005[i]	
$(\beta CD)_2$su	TNS^-	16.70 ± 0.02[i]		
$(\beta CD)_2$ox	TNS^-	32.64 ± 0.09[i]		
$(\beta CD)_2$ur	TNS^-	45.23 ± 0.07[i]		

[a] Errors represent one standard deviation. [b] Sum of the squares of the residuals. [c] Ref. 27. [d] From fitting for the equilibrium in eqn. (1). [e] From fitting for the equilibria in eqn. (1) and (2). [f] Ref. 26. [g] From fitting for the equilibrium in eqn. (5). [h] From fitting for the equilibria in eqn. (5) and (6). [i] Ref. 20.

$$\beta CD + MO^- \overset{K_1}{\rightleftharpoons} \beta CD \cdot MO^- \quad (3)$$

$$\beta CD \cdot MO^- + MO^- \overset{K_2}{\rightleftharpoons} \beta CD \cdot (MO)_2^{2-} \quad (4)$$

Complexation of TR^- by $(\beta CD)_2x$

The variations in the TR^- absorption spectrum with total $[(\beta CD)_2x]$ are exemplified by the montage shown in Fig. 4 for the $TR^-/(\beta CD)_2$su system. Those observed as total $[(\beta CD)_2$ur$]$ and $[(\beta CD)_2$ox$]$ are varied, are similar. An isosbestic point is observed at 526 nm [compared with 524 nm for the $TR^-/(\beta CD)_2$ur and 512 nm for $TR^-/(\beta CD)_2$ox systems, respectively.] These variations are consistent with the presence of two predominant environments for TR^- [eqn. (5)] where $(\beta CD)_2x \cdot TR^-$ is a host–guest complex. The fitting of the absorbance data for each system to the algorithm for the variation of TR^- absorption with total $[(\beta CD)_2x]$ for the equilibrium shown in eqn. (5), exemplified by the $TR^-/(\beta CD)_2$su system in Fig. 5, yields the K_1 values in Table 1.

$$(\beta CD)_2x + TR^- \overset{K_1}{\rightleftharpoons} (\beta CD)_2x \cdot TR^- \quad (5)$$

$$(\beta CD)_2x \cdot TR^- + TR^- \overset{K_2}{\rightleftharpoons} (\beta CD)_2x \cdot (TR)_2^{2-} \quad (6)$$

The absorption data for all three systems were fitted to the algorithm for the variation of TR^- absorption with total $[(\beta CD)_2x]$ arising from the combined equilibria shown in eqn. (5) and (6), and the derived K_1 and K_2 appear in Table 1. The errors in K_1 are greater than those derived when the data were fitted to the single equilibrium of eqn. (5), but the ssr are smaller. Over the total $[TR^-]$ and $[(\beta CD)_2x]$ ranges studied, the maximum percentages of TR^- existing in the free TR^-, $(\beta CD)_2x \cdot TR^-$ and $(\beta CD)_2x \cdot (TR)_2^{2-}$ environments as $[(\beta CD)_2x]$ is varied are 91.5, 91.3 and 2.7% for the $(\beta CD)_2$su system, 53.6, 94.1 and 43.5% for the $(\beta CD)_2$ox system and 84.0, 64.9 and 31.4% for the $(\beta CD)_2$ur system, as calculated from the simultaneously derived K_1 and K_2. On this basis, $(\beta CD)_2ox \cdot (TR)_2^{2-}$ and $(\beta CD)_2ur \cdot (TR)_2^{2-}$ appear to be significant species. However, the isosbestic points require the three environments for TR^- shown in the equilibria illustrated by eqn. (5) and (6) to produce identical absorbances for each of the three systems studied. This seems unlikely, and the formation of $(\beta CD)_2x \cdot TR^-$ as the greatly predominant species [eqn. (5)] appears the more plausible interpretation of

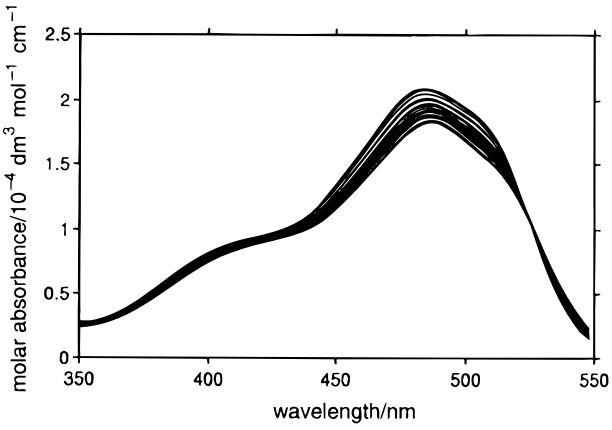

Fig. 4 Absorbance variation of TR^- (4.0×10^{-5} mol dm^{-3}) with $[(\beta CD)_2$su$]$ in the range (2.38×10^{-5})–(4.93×10^{-3}) mol dm^{-3} in aqueous phosphate buffer at pH 5.5 and 298.2 K. The TR^- absorbance decreases with increase in $[(\beta CD)_2$su$]$ from 350 nm to the isosbestic point beyond which it increases.

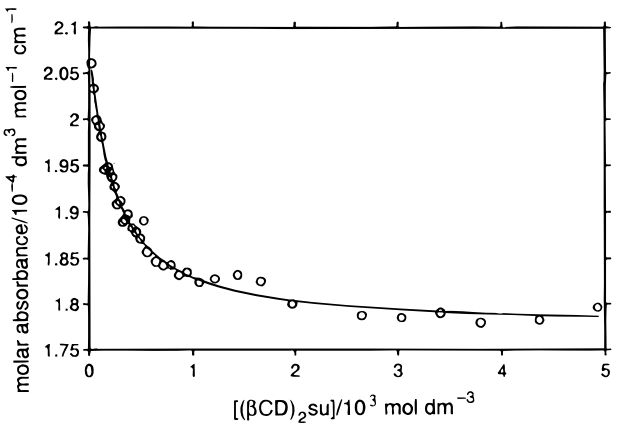

Fig. 5 Absorbance variation of TR^- with $[(\beta CD)_2$su$]$ at 480 nm under the same conditions as for Fig. 4. The solid curve represents the best fit of the data, collected at 2 nm intervals in the range 450–510 nm, to the algorithm arising from the equilibrium shown in eqn. (5).

the variation of the TR^- absorbance variation. Thus, $(\beta CD)_2x \cdot TR^-$ is much more stable than $\beta CD \cdot TR^-$, which is discussed below, and the strength of cooperative binding varies in the sequence $(\beta CD)_2ur \cdot TR^- > (\beta CD)_2ox \cdot TR^- > (\beta CD)_2su \cdot TR^-$.

For the formation of $\beta CD \cdot TR^-$ and $\beta CD \cdot (TR)_2^{2-}$

$$\beta CD + TR^- \overset{K_1}{\rightleftharpoons} \beta CD \cdot TR^- \quad (7)$$

$$\beta CD \cdot TR^- + TR^- \overset{K_2}{\rightleftharpoons} \beta CD \cdot (TR)_2^{2-} \quad (8)$$

$K_1 = (7.1 \pm 0.7) \times 10^2$ dm^3 mol^{-1} and $K_2 = (4 \pm 7) \times 10^6$ dm^3 mol^{-1}, respectively, as shown by temperature-jump spectroscopy under identical conditions to those used in this study.[26] The uncertainty in K_2 is very high, but the values of $K_1 = (4.18 \pm 1.47) \times 10^2$ dm^3 mol^{-1} and $K_2 = (1.68 \pm 0.54) \times 10^6$ dm^3 mol^{-1} for the analogous γCD are better determined and show similar relative orders of magnitude for K_1 and K_2. The relatively high value of K_2, by comparison with K_1, is attributed to the dimerization of TR^- ($K_{dimerization} = 910$ dm^3 mol^{-1}) being enhanced by γCD complexation.[26]

Discussion

It is seen (Table 1) that K_1 decreases in the sequence $(\beta CD)_2x \cdot MO^- > (\beta CD)_2x \cdot TNS^- > (\beta CD)_2x \cdot TR^-$ for each of the linkers, x, (Fig. 1) where TNS^- is 6-(*p*-toluidinyl) naphthalene-2-sulfonate.[20] [This discussion is confined to the formation of $(\beta CD)_2x \cdot G$ as shown in eqn. (1) and (5) for the reasons given above.] If the βCD moieties in $(\beta CD)_2x$ could act independently, $(\beta CD)_2x \cdot MO^{-1}$ should be twice as stable as $\beta CD \cdot MO^-$ on a statistical basis and the same relationship should exist for the analogous TNS^- and TR^- complexes. However, in all cases, K_1 for the $(\beta CD)_2x$ complex $\gg 2K_1$ for βCD, consistent with cooperative binding of the guest by the linked βCD moieties being the dominant complex stabilizing force. Accordingly, it is probable that variations in $(\beta CD)_2x \cdot G$ complex stability with change in guest largely reflect differences in interaction of the two aromatic binding groups of the guest with the linked βCD, and that changes in complex stability for a given guest with change in $(\beta CD)_2x$ reflect the extent to which the host–guest interactions approach optimization as the length of the linker changes.

The most strongly complexed guest is linear MO^-, whose flexibility is restricted by conjugation through the diazo linkage. This restriction may be a contributing cause of the increase in complex stability in the sequence $(\beta CD)_2su \cdot MO^- < (\beta CD)_2ur \cdot MO^- < (\beta CD)_2ox \cdot MO^{-1}$. Because $(\beta CD)_2ur$ has the shortest and least flexible linker, the two βCD moieties are probably less able to align their annuli to accommodate linear MO^- than is the more flexible $(\beta CD)_2ox$. However, while the longer linker in $(\beta CD)_2su$ leads to greater flexibility, the greater separation of the βCD moieties apparently does not allow them to accommodate both MO^- phenyl groups to maximize binding and complex stability decreases as a result. The second most strongly complexed guest, TNS^-, has a more extended aromatic system because of its naphthyl group and might be expected to interact more extensively with the hydrophobic interior of the βCD annulus. However, the rigidity of the naphthyl group seems to offset the flexibility gained from free rotation about the amine nitrogen of TNS^- so that it is less able to adapt to the steric restraints imposed in $(\beta CD)_2x \cdot TNS^-$ which is consequently less stable than $(\beta CD)_2x \cdot MO^-$. The least strongly complexed guest, TR^-, is also the most rigid and the most angular guest. [In the largely hydrophobic environment of $(\beta CD)_2x \cdot TR^-$, TR^- probably exists predominantly in the azo form shown in Fig. 1].[29,34] It appears that these properties render TR^- less able to adapt to the stereochemical constraints of $(\beta D)_2x$ so that $(\beta CD)_2x \cdot TR^-$ is less stable than its MO^- and TNS^- analogues. Thus, in the most stable complex, $(\beta CD)_2ox \cdot MO^-$, the interaction between the $(\beta CD)_2ox$ recognition sites and the MO^- binding sites is maximized and strain is minimized by comparison with the least stable complex, $(\beta CD)_2su \cdot TR^-$, in which the combination of these characteristics is less effective in stabilizing the complex.

We gratefully acknowledge the award of an Australian Postgraduate Research Award to C.A.H. and funding of this research by the University of Adelaide and the Australian Research Council. We thank Nihon Shokhuin Kako Co. Ltd. for a gift of βCD.

References

1 M. L. Bender and M. Komiyama, *Cyclodextrin Chemistry*, Springer Verlag, New York, 1978.
2 W. Saenger, *Inclusion Compounds*, 1984, **2**, 231.
3 R. J. Clarke, J. H. Coates and S. F. Lincoln, *Adv. Carbohydr. Chem. Biochem.*, 1989, **46**, 205.
4 K. Harata, *Inclusion Compounds*, 1991, **5**, 311.
5 S. E. Brown, J. H. Coates, C. J. Easton and S. F. Lincoln, *J. Chem. Soc., Faraday Trans.*, 1994, **90**, 739.
6 S. E. Brown, C. A. Haskard, C. J. Easton and S. F. Lincoln, *J. Chem. Soc., Faraday Trans.*, 1995, **91**, 1013, 4335.
7 K. Fujita, S. Ejima and T. Imoto, *J. Chem. Soc., Chem. Commun.*, 1984, 1277.
8 R. Breslow, N. Greenspoon, T. Guo and R. Zarzycki, *J. Am. Chem. Soc.*, 1989, **111**, 8296.
9 J. H. Coates, C. J. Easton, S. J. van Eyk, S. F. Lincoln, B. L. May, C. B. Walland and M. L. Williams, *J. Chem. Soc., Perkin Trans. 1*, 1990, 2619.
10 R. C. Petter, C. T. Sikorski and D. H. Waldeck, *J. Am. Chem. Soc.*, 1991, **113**, 2325.
11 B. Zhang and R. Breslow, *J. Am. Chem. Soc.*, 1992, **114**, 5882.
12 B. Zhang and R. Breslow, *J. Am. Chem. Soc.*, 1993, **115**, 9353.
13 R. Breslow, *Recl. Trav. Pay-Bas*, 1994, **113**, 493.
14 C. T. Sikorski and R. C. Petter, *Tretrahedron Lett.*, 1994, **35**, 4275.
15 F. Venema, C. M. Baselier, E. van Dienst, B. H. M. Ruël, M. C. Feiters, J. F. J. Engbersen, D. N. Reinhout and R. J. M. Nolte, *Tetrahedron Lett.*, 1994, **35**, 1773.
16 F. Venema, C. M. Baselier, M. C. Feiters and R. J. M. Nolte, *Tetrahedron Lett.*, 1994, **35**, 8661.
17 R. Deschenaux, A. Greppi, T. Ruch, H. P. Kriemler, F. Raschdorf and R. Ziessel, *Tetrahedron Lett.*, 1994, **35**, 2165.
18 Y. Wang, A. Ueno and F. Toda, *Chem. Lett.*, 1994, 167.
19 T. Jiang, D. K. Sukumaran, S. D. Soni and D. S. Lawrence, *J. Org. Chem.*, 1994, **59**, 5149.
20 C. A. Haskard, C. J. Easton, B. L. May and S. F. Lincoln, *J. Phys. Chem.*, 1996, **100**, 14457.
21 W. Broser, *Z. Naturforsch., Teil B*, 1953, **8**, 722.
22 H. Zollinger, *Azo and Diazo Chemistry: Aliphatic and Aromatic Compounds*, Interscience, New York, 1961.
23 J. Pitha and R. N. Jones, *Can. J. Chem.*, 1966, **44**, 3031.
24 F. Quadrifoglio and V. Crescenzi, *J. Colloid Interface Sci.*, 1971, **35**, 447.
25 R. L. Reeves, M. S. Maggio and S. A. Harkaway, *J. Phys. Chem.*, 1979, **83**, 2359.
26 R. J. Clarke, J. H. Coates and S. F. Lincoln, *J. Chem. Soc., Faraday Trans.*, 1984, **80**, 3119.
27 R. J. Clarke, PhD Thesis, University of Adelaide, 1985.
28 I. Tabushi, Y. Kuroda and T. Mizutani, *Tetrahedron*, 1984, **40**, 545.
29 Y. Matsui and K. Mochida, *Bull. Chem. Soc. Jpn.*, 1978, **51**, 673.
30 A. Buvari and L. Barcza, *J. Incl. Phenom.*, 1989, **7**, 313.
31 H-J. Schneider and F. Xiao, *J. Chem. Soc., Perkin Trans. 2*, 1992, 387.
32 R. I. Gelb and L. M. Schwartz, *J. Incl. Phenom. Mol. Recogn.*, 1989, **7**, 537.
33 K. M. Tawarah and A. A. Wazwaz, *Ber. Bunsen-Ges. Phys. Chem.*, 1993, **97**, 727.
34 R. L. Reeves and R. S. Kaiser, *J. Org. Chem.*, 1970, **35**, 3670.

Paper 6/03638D; *Received* 24*th May*, 1996